Acta Mechanica Sinica (2006) 22:409–416
DOI 10.1007/s10409-006-0020-y

RESEARCH PAPER

Study on micronozzle flow and propulsion performance using DSMC and continuum methods

Minghou Liu · Xianfeng Zhang · Genxuan Zhang · Yiliang Chen

Received: 28 December 2005 / Revised: 20 April 2006 / Accepted: 10 May 2006 / Published online: 28 July 2006

Abstract In this paper, both DSMC and Navier–Stokes computational approaches were applied to study micronozzle flow. The effects of inlet condition, wall boundary condition, Reynolds number, micronozzle geometry and Knudsen number on the micronozzle flow field and propulsion performance were studied in detail. It is found that within the Knudsen number range under consideration, both the methods work to predict flow characteristics inside micronozzles. The continuum method with slip boundary conditions has shown good performance in simulating the formation of a boundary layer inside the nozzle. However, in the nozzle exit lip region, the DSMC method is better due to gas rapid expansion. It is found that with decreasing the inlet pressure, the difference between the continuum model and DSMC results increases due to the enhanced rarefaction effect. The coefficient of discharge and the thrust efficiency increase with increasing the Reynolds number. Thrust is almost proportional to the nozzle width. With dimension enlarged, the nozzle performance becomes better while the rarefaction effects would be somewhat weakened.

Keywords Micronozzle · DSMC · Continuum model · Slip boundary condition · Thrust efficiency

The project supported by the National Natural Science Foundation of China (10372099). The English text was polished by Boyi Wang.

M. Liu (✉) · X. Zhang · G. Zhang · Y. Chen
Department of Thermal Science and Energy Engineering, University of Science and Technology of China, Hefei 230027, China
e-mail: mhliu@ustc.edu.cn

1 Introduction

Recently, there is a tendency toward shrinking fabrication and launch cost, and increasing reliability and multiformity in function. In order to obtain these objects, satellites' miniaturization and micromation have been rapidly developed. With development in MEMS (microelectric mechanical system), integrated micro satellite with "digital micropropulsion" has been developed to obtain the multifunctional satellite [1,2]. To complete the orbiting mission and to achieve stabilization, station-keeping and attitude-controlling, lower thrust (0.1–10 mN) and impulse bit are required, which could be completed by micropropulsion. One of the simplest forms of the micro propulsion is the cold gas thruster. The thrust is generated when a high pressure gas expands through a nozzle. Cold gas thrusters have small specific impulse (approximately 70 s). However, these systems are easy to use and to implement at a low cost. As one of the key components in a propulsion system, nozzle needs to be microminiaturized. There are some differences in flow field with conventional one due to the reduced characteristic dimension in the micronozzle. In a micro flow field, Reynolds number becoming small results in a large viscous loss, thicker boundary layer and reduced level of efficiency in micronozzle. At the same time there may be several flow regimes such as continuum flow, slip-flow regime and transition regime, even free-molecule flow regime because of higher Knudsen number inside micronozzle [3].

Experimental studies [4,5] showed that micronozzle's thrust efficiency and specific impulse efficiency would rapidly decrease when Reynolds number lower than 1,500. For a axisymmetric nozzle, there was fully viscous flow at a Reynolds number of about 1,000. As a result,

in the divergence section density of core flow increases and the velocity decreases. It is the reason that characteristic dimension diminished causes Reynolds number lessening, viscous dissipation strengthening, and wall boundary layer augment. Inlet chamber pressure of micronozzle would take effect on its performance. With chamber pressure increasing, the throat Reynolds number also increases and thrust coefficient and specific impulse are enhanced. Furthermore, it has been demonstrated that the variety of nozzle dimension directly affects thrust, thrust coefficient, specific impulse and nozzle coefficient of discharge as a function of throat Reynolds number [6].

In the micro-devices, continuous medium hypothesis is still applicable as Knudsen number is not too big. When Knudsen number exceeds 0.001 with decreasing dimension, there are some rarefaction effects such as velocity slip and temperature jump. To deal with these problems, Navier–Stokes equations are solved with slip-flow and temperature-jump boundary conditions [7]. However, Navier–Stokes equations with slip boundary conditions are no longer applicable as the Knudsen number exceeds 0.1. As a kind of micro flow, there are the same phenomena in the micronozzle flows. The continuum-based method is deficient in simulating highly rarified micro-nozzle flows [8]. The Direct Simulation Monte Carlo (DSMC) method has been intensively used to predict the flow field inside micro-devices and the corresponding propulsion performance [9–12].

In this paper, both the continuum and DSMC methods are applied to simulate the flow inside micronozzles. The effects of inlet condition, wall boundary condition (no-slip, slip), micronozzle dimension, Reynolds number and Knudsen number on micro-nozzle performance were studied in detail.

2 Numerical methods

2.1 DSMC method

The DSMC method in the variable hard sphere (VHS) collision model [13] was applied in the present work for the high speed, low Reynolds number micronozzle flows. Under the flow and geometry conditions examined in this work, gas-surface interactions are expected to affect the flow significantly. Hence, the Maxwell model was used to model gas-surface interaction. The momentum and thermal accommodation coefficients were assumed unity in this work.

The inlet pressure was fixed constant during this study. For the supersonic flow, the outlet pressure was given as 10 Pa for reference, the exact value was extrapolated. For the pressure boundary condition, Ikegawa and Nance [14,15] developed a method using the particle flux conservation concept by which the inlet velocity can be determined. This treatment method is complex and unstable. Hence the method proposed by Liou and Fang [16] was employed in this work. That is

$$(U_{\text{in}})_j = U_j. \tag{1}$$

And the inlet temperature (T_{in}) and number density (n_{in}) can be obtained from inlet pressure (p_{in}) and density (ρ_{in}). That is

$$(n_{\text{in}})_j = \frac{\rho_{\text{in}}}{m}, \tag{2}$$

$$(T_{\text{in}})_j = \frac{p_{\text{in}}}{\rho_{\text{in}} R}, \tag{3}$$

where R is the gas constant, m the molecular mass.

For the outlet boundary conditions the same treatment methods are applied. That is

$$(\rho_{\text{e}})_j = \rho_j + \frac{p_{\text{e}} - p_j}{(a_j)^2}, \tag{4}$$

$$(U_{\text{e}})_j = U_j + \frac{p_j - p_{\text{e}}}{\rho_j a_j}, \tag{5}$$

$$(V_{\text{e}})_j = V_j, \tag{6}$$

$$(T_{\text{e}})_j = \frac{p_{\text{e}}}{(\rho_{\text{e}})_j R}, \tag{7}$$

$$(n_{\text{e}})_j = \frac{\rho_{\text{e}}}{m}, \tag{8}$$

where U and V are the streamwise and normal velocities, a the local speed of sound, subscript "in" and "e", respectively, represent quantities at the inlet and exit boundary, subscript j the computed quantities in the jth cell. Then the particle number fluxes and the velocity components of entering molecules are determined locally from the Maxwellian distribution.

2.2 Continuum model

The Reynolds number based on nozzle throat width ($Re_t = UL_t/\nu$, where U and L_t are the streamwise velocity and nozzle throat width, respectively, ν is the kinetic viscosity) is less than 1,000, therefore, Navier–Stokes equation with laminar flow assumption was applied. Due to the nature of the problem, a two-dimensional simulation was used to evaluate the nozzle flow. The numerical calculation was for steady-state conditions through a finite volume simulation of compressible Navier–Stokes equation. In this work, the convection terms in all equations were discretized using the second-order up-wind interpolation scheme. The discretized equations were solved by the SIMPLE method. At the inlet boundary, total pressure and total temperature were given. At

the outlet boundary, the extrapolated conditions were given for the supersonic flow. The wall is adiabatic. Gas compressibility is considered and the dynamic viscosity coefficient is a function of temperature. The flow domain was discretized using 410 × 140 non-uniform quadrilateral elements. Through grid refinement we did not observe significant differences. We monitored this by observing various points in the domain. Finally, in all of the simulations we monitored errors in the integral form of the conservation laws. The absolute maximum errors in the mass, momentum and energy conservation equations are less than 0.05, 0.1 and 0.7%, respectively. The details of numerical validation can be found in [17].

Two kinds of wall boundary conditions are considered, which are no-slip condition and first-order slip condition, respectively. For an ideal gas with the wall temperature constant, the first-order slip boundary condition can be written as [7]

$$u_g - u_w = \frac{2-\sigma_v}{\sigma_v}\lambda\left(\frac{\partial u}{\partial y}\right)_w + \frac{3}{4}\frac{\mu}{\rho T_g}\left(\frac{\partial T}{\partial x}\right)_w. \tag{9}$$

Similar arguments are made for the temperature-jump boundary condition by von Smoluchowsi as follows:

$$T_g - T_w = \frac{2-\sigma_T}{\sigma_T}\left(\frac{2\gamma}{\gamma-1}\right)\frac{\lambda}{Pr}\left(\frac{\partial T}{\partial y}\right)_w, \tag{10}$$

where x and y are respective the streamwise and normal coordinates, ρ and μ are the gas density and viscosity, u and T are the gas velocity and temperature, the subscript g and w, respectively, stand for gas adjacent to wall and wall, λ the gas mean free path, γ the specific heat ratio, Pr the Prandtl number, σ_v and σ_T are the tangential momentum accommodation coefficient and the thermal accommodation coefficient, respectively. According to investigation of DSMC method [8], σ_v and σ_T here are equal to 1.

3 Results and discussion

In present study, a 2D micronozzle with the throat width 30 μm as the benchmark is shown in Fig. 1, where L_{in} and L_{out} are the inlet and outlet width, respectively, L_t the throat width, L_1 and L_2 the interval from throat to inlet and outlet, R the semi-diameter of throat arc, θ_1 and θ_2 the half convergence angle and half divergence angle. When the half divergence angle is about 20 and ratio of L_t and L_{out} about 5, the performance of micronozzle is optimal [17,18]. And the micronozzle as the benchmark is that: $L_{\text{in}} = 70\,\mu\text{m}$, $L_{\text{out}} = 138\,\mu\text{m}$, $R = 50\,\mu\text{m}$, $L_1 = 48\,\mu\text{m}$, $L_2 = 157\,\mu\text{m}$, $\theta_1 = 30°$, $\theta_2 = 20°$. In all cases of this paper, inlet boundary conditions are the pressure inlet, the temperature of the incoming nitrogen gas and the walls are 300 K and exit pressure is 10 Pa constant for reference. In order to save computation time, only half flow field domain is computed because of the symmetry of nozzle geometry.

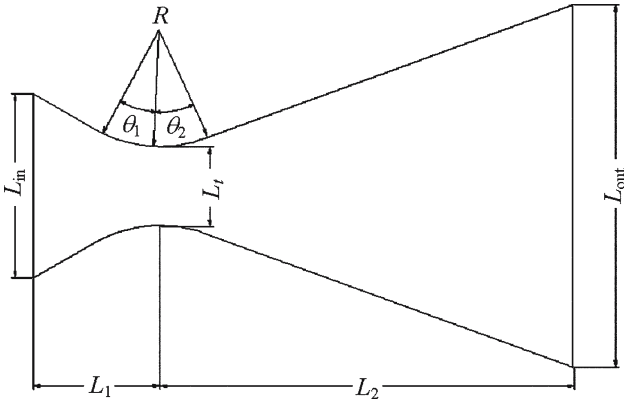

Fig. 1 Micronozzle configuration

3.1 Comparisons between DSMC and continuum methods

The local Knudsen number contours are plotted in Fig. 2, which are obtained by DSMC with the inlet pressure 1 atm. In the nozzle, the Knudsen number ranges from 0.0088 to 0.026 and there are two flow regimes: the continuum flow and slip-flow regime. When the continuum method is applied, the slip boundary condition should be considered due to Knudsen number exceeds 0.001 in most nozzle region.

Figure 3 shows the Mach number contours for micronozzle obtained by DSMC and the continuum method with slip boundary condition at 1 atm of the inlet pressure. The results of two methods agree well with each other inside the nozzle. The features of the nozzle flow include the formation of a boundary layer inside the nozzle and rapid expansion as the flow travels past the

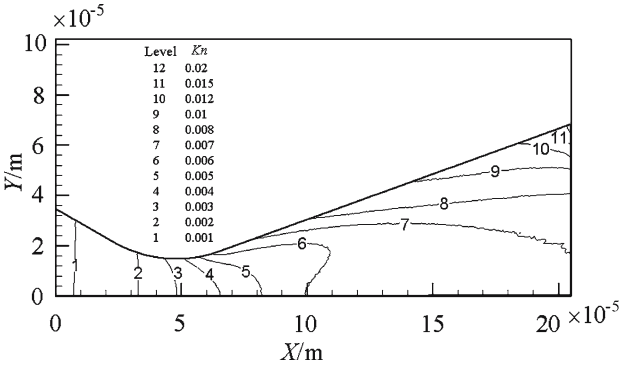

Fig. 2 The local Knudsen number contours for the micronozzle

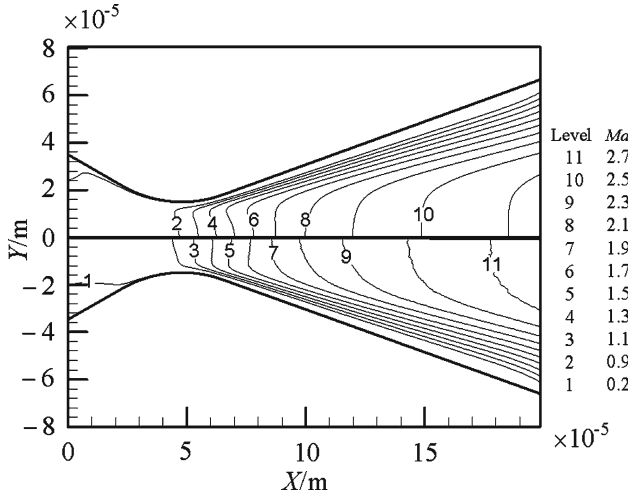

Fig. 3 Mach number contours for micronozzle obtained by DSMC (*bottom*) and slip (*top*)

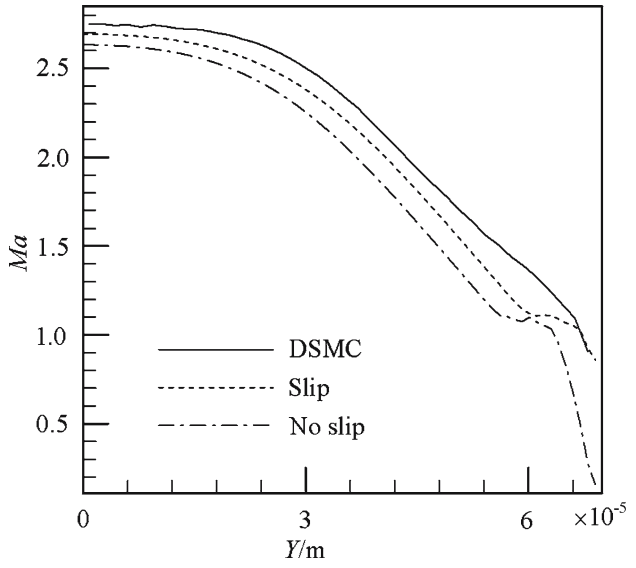

Fig. 5 Mach number profile at the exit plane with $P_i = 0.5$ atm

micronozzle lip at the exit. Inside the nozzle, effects of boundary layer play an important role in determining the nozzle flow characteristics. For the Knudsen number we applied, both DSMC and the continuum method with slip boundary condition can predict flow well. However, with rapid expansion in the region of nozzle exit lip, the gas becomes rarefied. As a result, the results of continuum method show a little difference compared with ones of DSMC method (Fig. 3). Figures 4, 5 and 6 show Mach number profiles at the exit plane for different inlet pressure (P_i). It is found that with decreasing inlet pressure, the results difference increases due to the rarefaction effect. For the three inlet pressure cases, the results of DSMC are the biggest, while continuum method with no slip boundary conditions gives the smallest. For case of 1 atm inlet pressure (Fig. 4), the results of DSMC and the continuum methods fit best than other two cases (Figs. 5, 6). Mach number profile along the nozzle centerline with $P_i = 0.5$ atm is shown in Fig. 7. They agree well with each other except near the exit. There is a more significant difference between these methods at $P_i = 0.1$ atm in the nozzle exit lip regions. Temperature profile along the centerline at $P_i = 0.1$ atm is given in Fig. 8. When the local Knudsen number is equal to 0.045 at $X = 8 \times 10^{-5}$ m, the results of continuum method with slip condition begin to deviate from ones of DSMC. It is because when inlet pressure drops, rarefaction effect

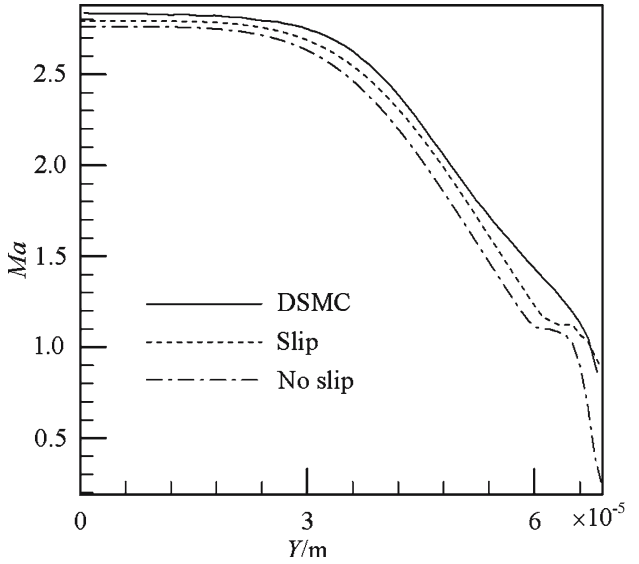

Fig. 4 Mach number profile at the exit plane with $P_i = 1$ atm

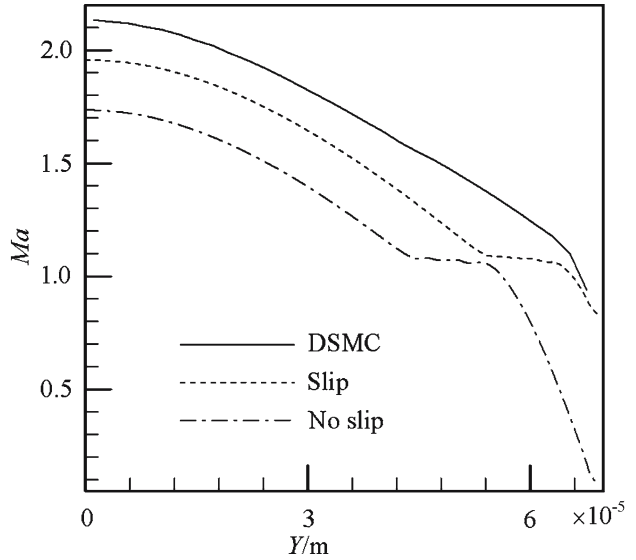

Fig. 6 Mach number profile at the exit plane with $P_i = 0.1$ atm

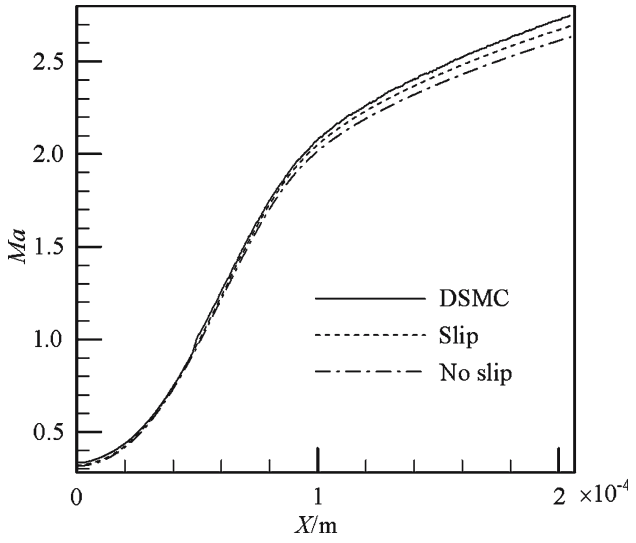

Fig. 7 Mach number profile along the centerline with $P_i = 0.5$ atm

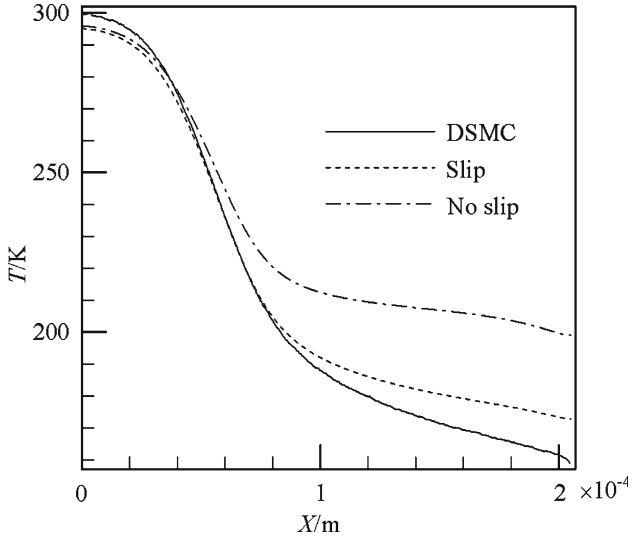

Fig. 8 Temperature profile along the centerline with $P_i = 0.1$ atm

increases. The flow reaches the transitional regime. The validity of Navier–Stokes solutions must be reevaluated.

3.2 The study on micronozzle performance

For a micronozzle, thrust and specific impulse (I_{sp}) are essential parameters to access the performance. Thrust F_t and thrust per unit mass flow rate I_{sp} are defined as follows:

$$F_t = \int_0^{L_{\mathrm{out}}} (\rho_{\mathrm{e}} u_{\mathrm{e}}^2 + p_{\mathrm{e}}) h_0 \, \mathrm{d}y, \qquad I_{\mathrm{sp}} = \frac{F_t}{\dot{m} g}, \tag{11}$$

where ρ_{e}, u_{e} and p_{e} are the outlet values of density, velocity and pressure, respectively, $\dot{m}$ the mass flow rate, g the gravity acceleration and h_0 the nozzle height. In addition, coefficients of discharge (C_d) and thrust efficiency (η_f) are used to access the nozzle efficiency, and defined as

$$\eta_f = \frac{F_{\mathrm{numerical}}}{F_{\mathrm{ideal}}}, \quad C_d = \frac{\dot{m}_{\mathrm{numerical}}}{\dot{m}_{\mathrm{ideal}}}, \tag{12}$$

where the subscript "ideal" represents the corresponding quasi 1-D prediction of inviscid nozzle performance.

The influence of the Reynolds number on micronozzle flow and micro nozzle's thrust performance is studied in this subsection. The predictions of micronozzle performance from the DSMC method are given under different inlet pressures in Table 1. With the inlet pressure increasing from 0.1 to 2 atm, the throat Reynolds number (Re_t) and thrust increase nearly linearly. Because of viscous loss decreasing and weakened blockage of throat, coefficient of discharge and thrust efficiency also increase accordingly. Worthwhile, the specific impulse I_{sp} increase more slowly than the thrust efficiency η_f with increasing the pressure ratio. In these test cases, relative difference of I_{sp} between the maximal and the minimum is 11.2% while 21.94% for thrust efficiency. According to definition, the specific impulse is nearly proportional to the nozzle exit velocity and thrust efficiency is proportional to the square of the exit velocity. For the quasi 1-D inviscid supersonic flow, velocity is only related with the micronozzle configuration and the inlet temperature. In these cases, the micronozzle configuration and inlet temperature are fixed. Hence, it is concluded that nozzle performance can be considered as a function of the Reynolds number. With increasing of the Reynolds number, better nozzle performance can be achieved due to the decreased blockage and the lessened viscous losses.

Figure 9 shows the effective area ratio from the throat to the exit for different inlet pressure. Due to the blockage of boundary layer and the viscous stresses at the low Reynolds numbers, effective area ratio is less than the real area ratio. Furthermore, the effective area ratio decreases with decreasing the inlet pressure due to the enlarged blockage, which diminishes to only 60% of geometry area ratio at $P = 0.1$ atm.

Keeping the micronozzle configuration and changing the length size, several cases with different throat width: $L_t = 3, 6, 15$, and $30\,\mu$m are simulated by the DSMC method with the inlet pressure fixed to its atmospheric value. It is found that the Mach number in the divergence section of the nozzle increases with increasing the throat width, which is shown in Fig. 10. Note that X^* is the non-dimensional length normalized by the half throat

Table 1 Performance parameters at different inlet pressures

P_i/atm	Re_t	C_d	F_t/mN	η_f	I_{sp}/s
0.1	44.3	0.8572	0.1112	0.7457	61
0.5	229.7	0.9180	0.6225	0.8771	66.2
1	462.8	0.9771	1.3565	0.9432	67.7
2	979.6	0.9802	2.7479	0.9553	68.7

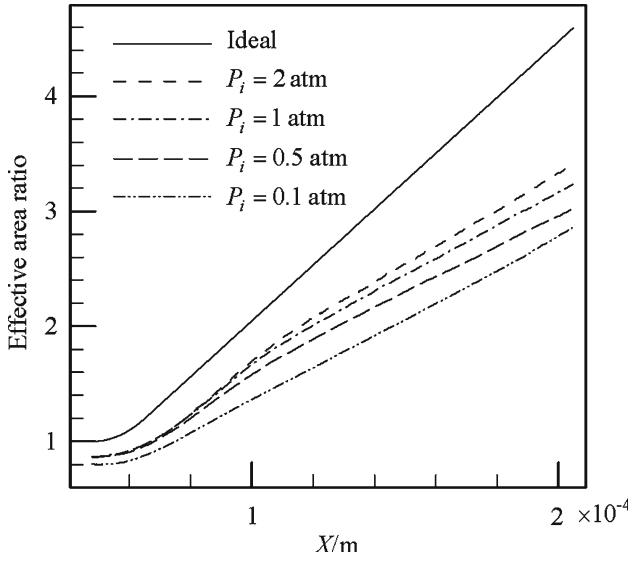

Fig. 9 Effective area ratio at the different inlet pressures

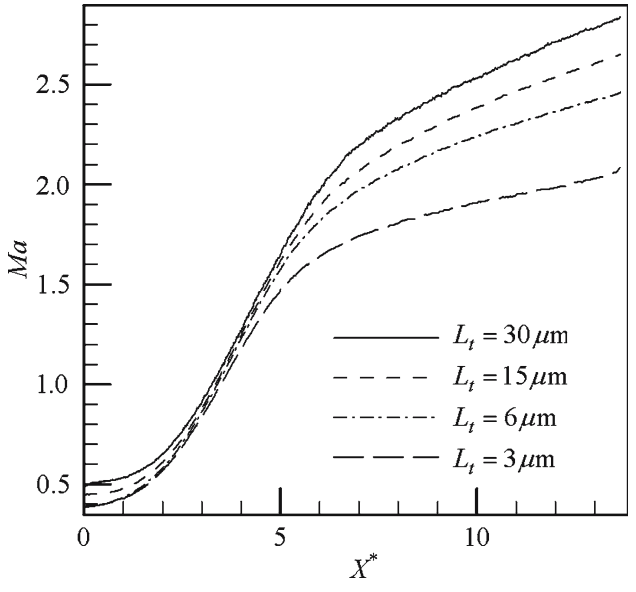

Fig. 10 Mach number profile along the centerline of the micronozzle for different throat widths

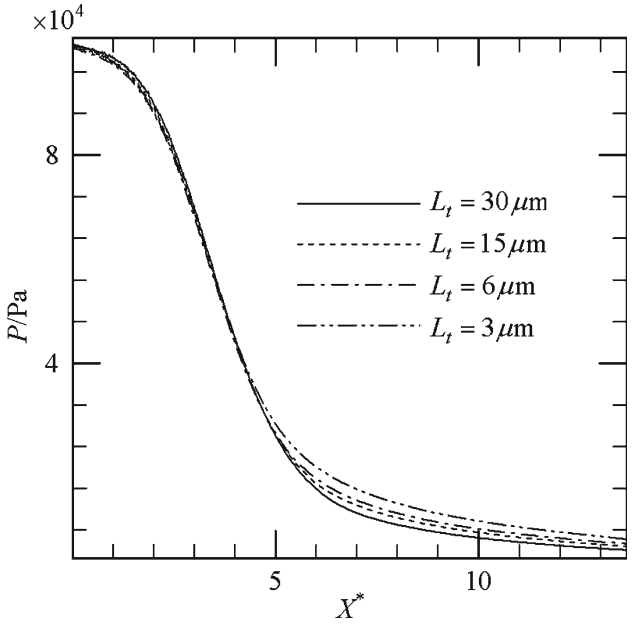

Fig. 11 Pressure profile along the centerline of the micronozzle for different throat widths

width. Figure 11 shows the pressure distributions along the centerline of the nozzle for different throat widths. With the nozzle configuration fixed, the pressure along the centerline is not very sensitive to the nozzle width, except for the nozzle exit lip region, where the larger throat width leads to a slight decreasing of the centerline pressure. Both of the increased outlet Mach number and decreased outlet centerline pressure effects indicate that the nozzle thrust would significantly increase with increasing the throat width.

Table 2 lists the corresponding micronozzle performance parameters for all test cases here. It is seen that the thrust is almost proportional to the nozzle width. Worthwhile, all the values of the corresponding efficiency, which represents the nozzle performance, increase with increasing the nozzle throat width due to the smaller viscous loss. Furthermore, the specific impulse still increases more slowly than the thrust efficiency due to the increased coefficient of discharge caused by the weakened blockage, which has been discussed in detail in the previous paragraph.

Till now, it has been found that the nozzle propulsion performance can be improved by either increasing the inlet pressure or increasing the throat width. Worthwhile, both approaches in changing the work conditions

Table 2 Performance parameters for different throat widths

L_t/μm	C_d	F_t/mN	η_f	I_{sp}/s
3	0.8269	0.106	0.7371	62.5
6	0.866	0.2284	0.7940	64.3
15	0.9383	0.636	0.8844	66.1
30	0.9771	1.3565	0.9432	67.7

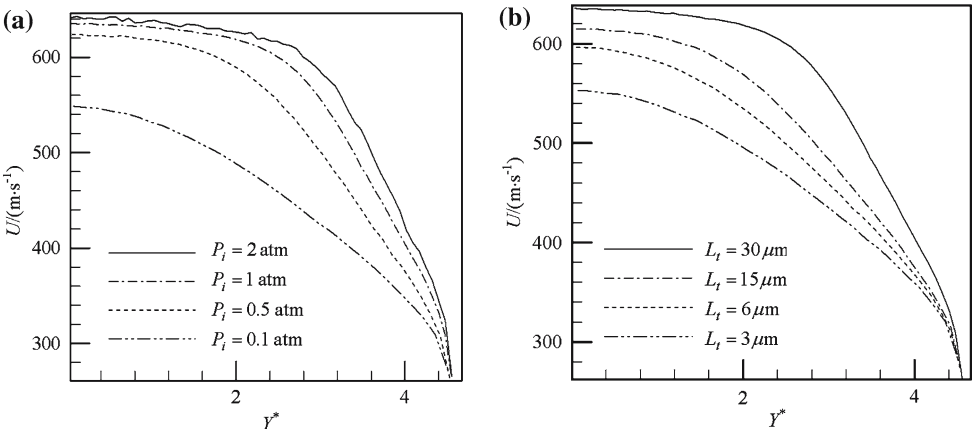

Fig. 12 Velocity profile at the exit plane for different inlet pressures (**a**) and different throat widths (**b**). **a** $L_t = 15\,\mu$m; **b** $P_i = 1$ atm

have shown similar trends for the influence of the Reynolds number on the nozzle performance. Therefore, it is apparently concluded that it is the increased Reynolds number that represents the weakened blockage and the smaller viscous loss and thus improves the nozzle performance.

It should be pointed out that when keeping the inlet pressure constant, the outlet boundary pressures are different for different throat widths (Fig. 11). As we mentioned above, for the supersonic flow, the outlet boundary pressure is extrapolated from inside flow. When dimension is reduced, the rarefaction effect is enhanced. Therefore, pressure drop due to surface friction is diminished. Keeping the inlet pressure constant, the nozzle with wider throat width gets higher the outlet pressure (Fig. 11).

Figure 12a shows the exit velocity profiles for different inlet pressures. Keeping nozzle throat width constant, higher inlet pressure results in bigger exit velocity. While keeping the inlet pressure constant, the exit velocity will increase in the micro nozzle with a broader throat width (Fig. 12b). Both approaches in changing the work conditions have shown similar trends for the influence of the Reynolds number of the nozzle flows. It is concluded that the nozzle exit velocities are increased by either increasing the inlet pressure or increasing the throat width due to enlarged Reynolds number, weakened rarefaction effect. Therefore, better nozzle propulsion performance can be achieved.

4 Conclusion

The DSMC and continuum-based methods were used to simulate the micronozzle flow with different nozzle dimensions and the inlet pressures in this paper. Simulations of relatively small Knudsen number flows based on these two methods have been demonstrated to agree well with each other except for the nozzle exit lip region. However, the continuum-based results were shown obvious deviations from the DSMC results as *Kn* exceeds 0.045.

It is concluded that the 2D cold gas micronozzle propulsion performance can intuitively be considered as a function of the Reynolds number. The coefficient of discharge and the thrust efficiency have been demonstrated to increase with increasing the Reynolds number. For a given nozzle, the Reynolds number and the thrust increase nearly linearly with the inlet pressure. When the micronozzle geometry and the inlet pressure are fixed, the thrust exhibits an approximately linear relationship with the throat width. It is also found that the specific impulse is not as sensitive as thrust efficiency on the throat width. In general, the Knudsen number is a key parameter to examine the validity of continuum models, while the Reynolds number is demonstrated as another important parameter to indicate the nozzle propulsion performance. And both of the Knudsen number and the Reynolds number distinctly affect the micronozzle flow field.

References

1. Rossi, C.: Micropropulsion for space – a survey of mems-based micro thrusters and their solid propellant technology. Sensors Updates **10**, 257–292 (2002)
2. Lewis, D., Janson, S., Become, R., Antonsson, E.: digital micropropulsion. Sensors Actuat. A Phys. **80**, 143–154 (2000)
3. Ketsdever, A.D., Clarbough, M., Gimelshein, S.F., Alexeenko, A.A.: Experimental and numerical determination of micropropulsion device efficiencies at low Reynolds numbers. J. AIAA **43**(3), 633–641 (2005)
4. Bayt, R.L.: Analysis, fabrication and testing of a MEMS-fabricated micronozzles. PhD Thesis. MIT, Cambridge (1999)
5. Choudhuri, A.R., Barid, B., Gollahalli, S.R.: Effects geometry and ambient pressure on micronozzle flow. AIAA paper 2001–3331, Salt Lake City, Utah (2001)
6. Reed, B.: Decomposing solid micropropulsion nozzle performance issues. AIAA paper 2003-0672, Reno, Nevada (2003)
7. Gad-el-Hak, M.: The fluid mechanics of microdevices – the freeman scholar lecture. J. Fluids Eng. **121**, 5–33 (1999)
8. Alexeenko, A., Collins, R.J., Gimelshein, S.F., Levin, D.A.: Challenges of three-dimensional modeling of microscale propulsion devices with the DSMC method. In: Proceedings of 22nd symposium on rarefied gas dynamics, Sydney, Australia (2000)
9. Piekos, E.S., Breuer, K.S.: Numerical modeling of micromechanical devices using the direct simulation Monte Carlo method. J. Fluids Eng. **118**, 464–469 (1996)
10. Markelov, G.N., Ivanov, M.S.: Numerical study of 2D/3D micronozzle flows. AIP Conf. Proc. **585**(1), 539–546 (2001)
11. Wang, M.R., Li, Z.X.: Numerical simulations on performance of MEMS-based nozzles at moderate or low temperatures. Microfluidics Nanofluidics, **1**, 62–70 (2004)
12. Bird, G.A.: Molecular Gas Dynamics and the Direct Simulation of Gas Flows. Clarendon Press, Oxford (1994)
13. Shen, C.: Rarefied Gas Dynamics. Fundamentals, Simulation and Micro Flows. Springer, Berlin Heidelberg New York (2005)
14. Ikegawa, M., Kobayashi, J.: Development of a rarefied flow simulator using the DSMC method. JSME Int. J. **30**, 463–467 (1990)
15. Nance, R.P., Hash, D.B., Hassan, H.A.: Role of boundary conditions in Monte Carlo simulation of MEMS devices. J. Thermalphys. Heat Transfer **12**, 447–449 (1998)
16. Liou, W.W., Fang, Y.: Implicit boundary conditions for direct simulation Monte Carlo method in MEMS flow predictions. Comput. Model. Eng. Sci. **4**, 119–128 (2000)
17. Zhang, G.X., Cai, X.D., Liu, M.H., Chen, Y.L.: Cold flow field and propulsive performance of a micro laval nozzle (in Chinese). J. Propulsion Technol. **25**, 54–57 (2004)
18. Bayt, R.L., Breuer, K.S.: Viscous effects in supersonic mems-fabricated micronozzles. In: Proceedings of the 1998 ASME International Mechanical Engineering Congress and Exposition, Anaheim (1998)